



Article

Inhibition of p300/CBP-Associated Factor Attenuates Renal Tubulointerstitial Fibrosis through Modulation of NF- κ B and Nrf2

Sungjin Chung ¹, Soojeong Kim ², Mina Son ¹, Minyoung Kim ¹, Eun Sil Koh ¹,
Seok Joon Shin ¹, Cheol Whee Park ¹ and Ho-Shik Kim ^{2,*}

¹ Department of Internal Medicine, College of Medicine, The Catholic University of Korea, 222, Banpo-daero, Seocho-gu, Seoul 06591, Korea; chungs@catholic.ac.kr (S.C.); sma0917@naver.com (M.S.); gomy33@naver.com (M.K.); fiji79@catholic.ac.kr (E.S.K.); imkidney@catholic.ac.kr (S.J.S.); cheolwhee@hanmail.net (C.W.P.)

² Department of Biochemistry, College of Medicine, The Catholic University of Korea, 222, Banpo-daero, Seocho-gu, Seoul 06591, Korea; soojeong107@hanmail.net

* Correspondence: hoshik@catholic.ac.kr; Tel.: +82-2-2258-7294

Received: 14 March 2019; Accepted: 24 March 2019; Published: 28 March 2019



Abstract: p300/CBP-associated factor (PCAF), a histone acetyltransferase, is involved in many cellular processes such as differentiation, proliferation, apoptosis, and reaction to cell damage by modulating the activities of several genes and proteins through the acetylation of either the histones or transcription factors. Here, we examined a pathogenic role of PCAF and its potential as a novel therapeutic target in the progression of renal tubulointerstitial fibrosis induced by non-diabetic unilateral ureteral obstruction (UUO) in male C57BL/6 mice. Administration of garcinol, a PCAF inhibitor, reversed a UUO-induced increase in the renal expression of total PCAF and histone 3 lysine 9 acetylation and reduced positive areas of trichrome and α -smooth muscle actin and collagen content. Treatment with garcinol also decreased mRNA levels of transforming growth factor- β , matrix metalloproteinase (MMP)-2, MMP-9, and fibronectin. Furthermore, garcinol suppressed nuclear factor- κ B (NF- κ B) and pro-inflammatory cytokines such as tumor necrosis factor- α and IL-6, whereas it preserved the nuclear expression of nuclear factor erythroid-derived 2-like factor 2 (Nrf2) and levels of Nrf2-dependent antioxidants including heme oxygenase-1, catalase, superoxide dismutase 1, and NAD(P)H:quinone oxidoreductase 1. These results suggest that the inhibition of inordinately enhanced PCAF could mitigate renal fibrosis by redressing aberrant balance between inflammatory signaling and antioxidant response through the modulation of NF- κ B and Nrf2.

Keywords: histone acetyltransferase; p300/CBP-associated factor; kidney fibrosis; inflammation; oxidative stress; apoptosis

1. Introduction

The DNA double helix in eukaryotic cells is packaged into a compact structure called chromatin with the assistance of two major classes of proteins: histones and non-histones [1]. Among the histones, H1 is known as the linker histone while H2A, H2B, H3, and H4 are considered core histones. Each core histone has a flexible N-terminal tail that consists of amino acids prone to posttranslational modifications including acetylation, methylation, phosphorylation, ubiquitylation, sumoylation, ribosylation, citrullination, deamination, and proline isomerization [1]. These histone modifications play an important role in assembling heterochromatin and maintaining gene boundaries between transcribed and non-transcribed genes. Histone acetylation and deacetylation, orchestrated by histone acetyltransferase (HAT) and histone deacetylases (HDAC), respectively, regulate the opening and

closing of the chromatin structure to guide gene expression machinery [2]. Acetylation of histone by HATs results in the relaxation of the chromatin structure, which promotes gene expression, whereas the removal of the acetyl group by HDACs represses gene expression [1,3]. HATs are also known to be responsible for the accessibility of transcription factors and transcriptional activation [4,5]. Physiological equilibrium of histone acetylation is often disturbed by histone hyperacetylation caused by either HAT activity or lack of HDAC activity [1,3]. In some instances, histone hyperacetylation may result in the overexpression of genes unfavorable for cell survival. Previous studies have demonstrated that dysregulation of histone acetylation is linked to several diseases including cancer, neurodegenerative disease, and chronic inflammation [6,7].

HATs can be grouped into four families according to sequence homology and structural features as well as functions [1]: the Gcn5-related N-acetyltransferase (GNAT) family, MYST (MOZ, Ybf2, Sas2, and Tip60) family, p300/CBP family, and nuclear coactivators (NRC) family. HATs belonging to the GNAT family are associated with the acetylation of lysine residues on histones H2B, H3, and H4 [1]. As a member of the GNAT family, p300/CBP-associated factor (PCAF) is involved in the regulation of cell transcription, progression, and differentiation [1,8]. For PCAF activity, lysines (K) 9 and 14 of histone H3 are preferred substrates [8]. PCAF can also bridge transcriptional factors to the transcriptional complex to provide appropriate levels of gene activities in cells in response to extracellular stimuli [9]. To date, some studies have suggested that PCAF can regulate the expression of inflammatory molecules [1,5,9,10]. PCAF has been reported as one of the genes significantly regulated by activated protein C in human macrophages [4]. Importantly, PCAF is considered to play a role in microglial inflammation through acetylation-dependent nuclear factor kappa B (NF- κ B) activation [7].

Renal fibrosis involves a complex multistage process that is orchestrated by a network of cytokines, chemokines, growth factors, adhesion molecules, and signaling processes [10]. A few studies have shown that PCAF is associated with increased apoptosis and upregulation of some inflammatory genes such as intercellular adhesion molecule-1, vascular cell adhesion molecule-1, and monocyte chemoattractant protein-1 as well as NF- κ B in the kidneys of streptozotocin-induced diabetes rats, *db/db* mice, and lipopolysaccharide (LPS)-injected mice [2,11]. Oxidative stress is also implicated in the pathogenesis of various forms of renal injury [12,13]. However, little is known about the involvement of PCAF in oxidative stress in the pathogenesis of renal fibrosis. Therefore, the objective of this study was to evaluate whether PCAF might be involved in the regulation of epithelial-mesenchymal transition (EMT), oxidative stress, and inflammatory molecules in the kidneys of nondiabetic mice with unilateral ureteral obstruction (UUO). In addition, mechanisms of renal protection by garcinol, a PCAF inhibitor, were investigated in this study. Identifying additional roles of PCAF and epigenetic effects on renal fibrosis may further increase the possibility of developing therapeutic strategies against renal diseases.

2. Results

2.1. Expression Levels of PCAF and Histone Acetylation in Kidneys Are Increased after UUO

We initially tested whether UUO surgery could cause changes in PCAF expression in obstructed kidneys. Immunohistochemistry analysis and immunoblotting showed that PCAF staining in kidneys was markedly increased on both days 3 and 7 after UUO when compared to that in the kidneys of sham-operated mice (Figure 1A–D). Such elevation in PCAF expression was reduced by the PCAF inhibitor garcinol. Consistent with results of PCAF expression, acetylation of K9 on histone H3 (H3K9ac) was also increased in obstructed kidneys. Such an increase was attenuated by garcinol treatment, where the finding was remarkable at day 7 after UUO (Figure 1E,F).

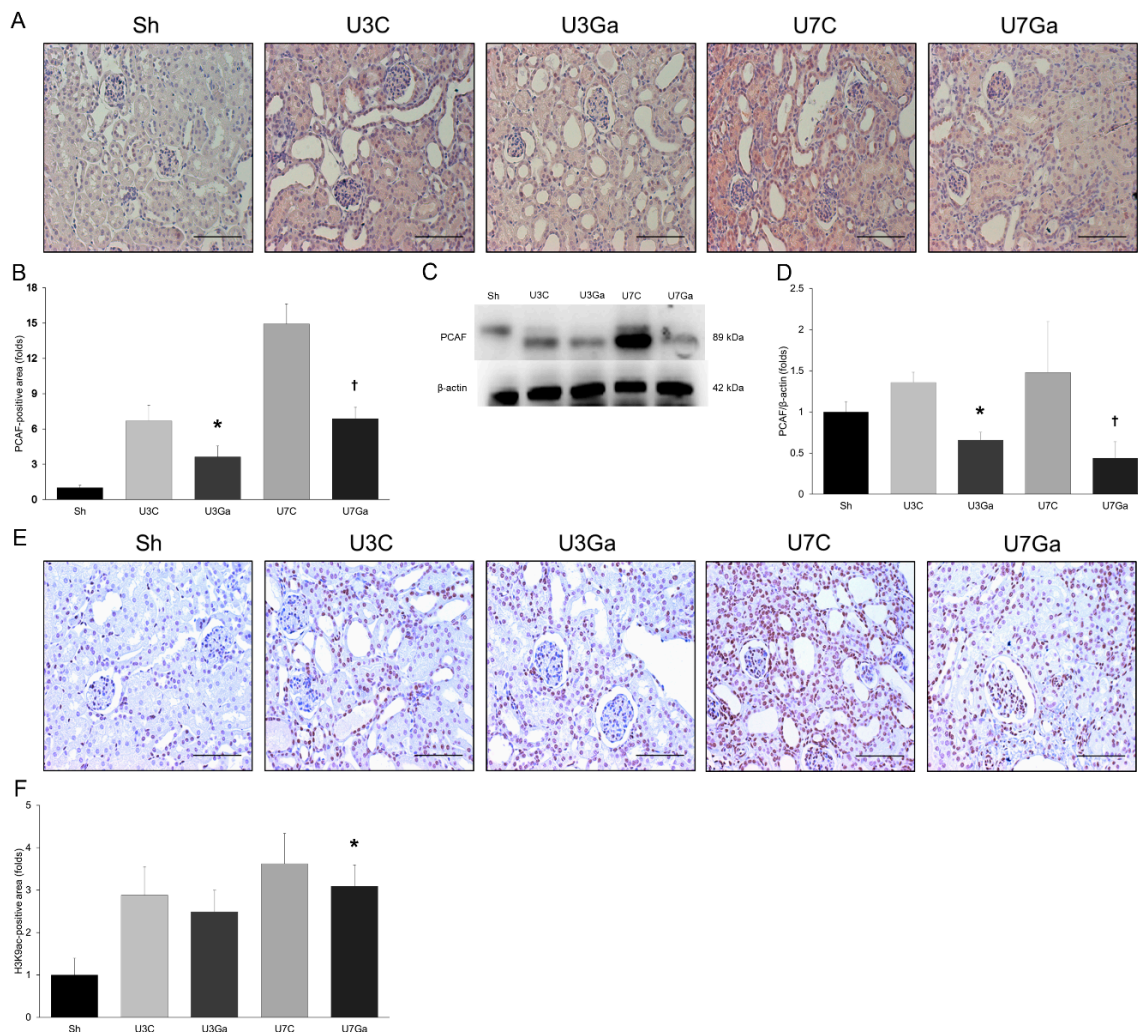


Figure 1. Renal expression of PCAF and H3K9ac with or without garcinol treatment after UUU. (A,B) Immunohistochemical staining and quantitative analysis showed the expression of PCAF increased in obstructed kidneys was decreased by garcinol treatment (scale bar, 2 μ m). * $p = 0.006$ vs. U3C, † $p < 0.001$ vs. U7C. (C,D) Representative Western blot showed that increased renal expression of PCAF in UUU-operated mice was decreased after garcinol treatment. * $p = 0.006$ vs. U3C, † $p < 0.001$ vs. U7C. (E,F) Immunohistochemical staining for H3K9ac demonstrated that the expression of H3K9ac elevated after UUU was attenuated by garcinol treatment (scale bar, 2 μ m). * $p = 0.044$ vs. U7C.

2.2. Inhibition of PCAF Leads to Attenuation of Fibrotic Changes in Obstructed Kidneys

Based on Masson's trichrome staining, renal tubulointerstitial fibrosis was increased after UUU when compared with that of the sham-operated mice. However, garcinol treatment significantly reduced fibrotic lesions after obstructive injury (Figure 2A,B). Total collagen content and type IV collagen (Col IV) expression in obstructed kidneys were significantly increased after UUU. Both were effectively decreased by garcinol treatment (Figure 2C–E). Garcinol administration also reduced the expression increase of transforming growth factor (TGF)- β 1 induced by UUU (Figure 2D,F,G). Collectively, these results indicate that PCAF plays a role in the progression of kidney fibrosis.

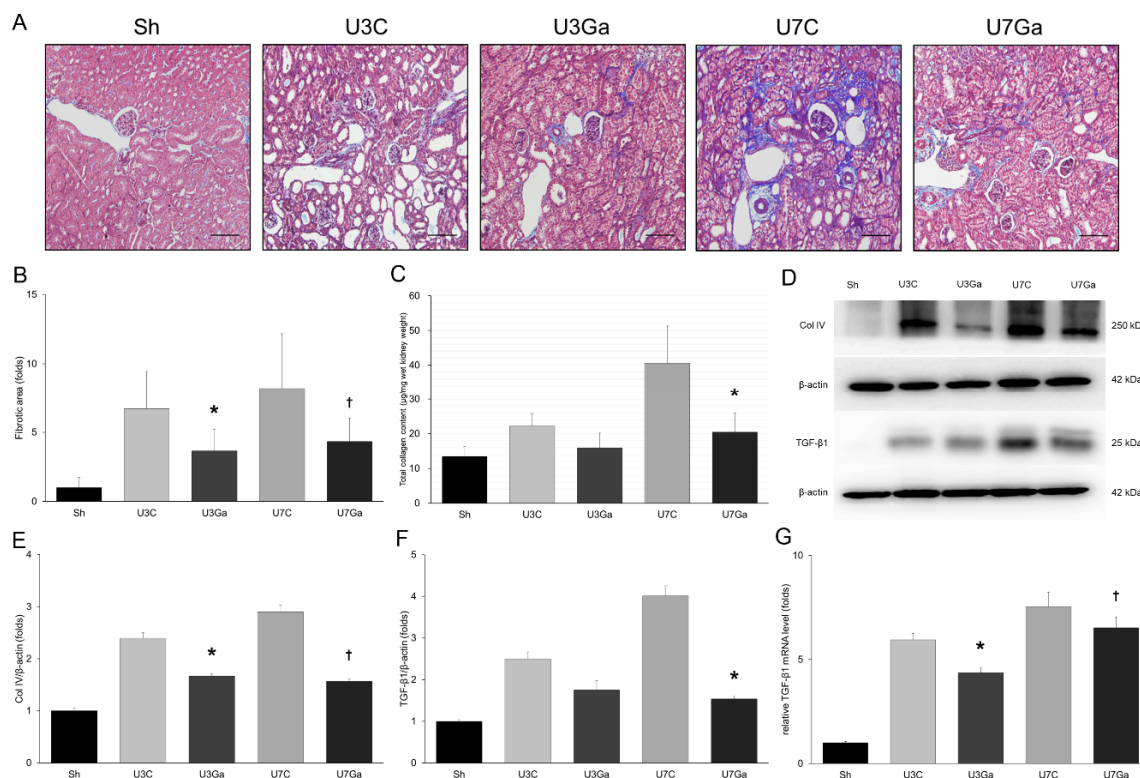


Figure 2. Effect of garcinol treatment on renal tubulointerstitial fibrosis after UUO. (A,B) Representative micrograph of Masson's trichrome staining showed that marked increase in renal fibrotic lesions after UUO was attenuated by garcinol treatment (scale bar, 2 μ m). * $p < 0.001$ vs. U3C, † $p < 0.001$ vs. U7C. (C) Renal total collagen content at day 7 post-UUO was significantly lower after garcinol treatment. * $p = 0.001$ vs. U7C. (D) Western blot for renal Col IV and TGF- β 1. (E) Quantitative analysis showed that renal Col IV level was decreased after garcinol treatment. * $p = 0.015$ vs. U3C, † $p < 0.001$ vs. U7C. (F) Protein expression of TGF- β 1 was attenuated by garcinol treatment at day 7 after UUO. * $p < 0.001$ vs. U7C. (G) mRNA level of TGF- β 1 was decreased by garcinol treatment in UUO kidneys. * $p = 0.001$ vs. U3C, † $p = 0.003$ vs. U7C.

2.3. Inhibition of PCAF Debilitates Epithelial-Mesenchymal Transition in Obstructed Kidneys

Renal tubular epithelial cells of patients with chronic kidney disease (CKD) undergo an EMT while increased expression of fibroblast-associated proteins and matrix deposition contribute to renal fibrosis [14]. Immunohistochemical staining revealed that levels of α -smooth muscle actin (α -SMA), a specific marker for myofibroblast activation, were significantly decreased in obstructed kidneys on both days 3 and 7 after the administration of garcinol (Figure 3A,B). Results of quantitative real-time polymerase chain reaction (qRT-PCR) revealed that increases in renal mRNA levels of α -SMA, vimentin, and fibronectin were significantly reduced by garcinol treatment at day 3 after UUO (Figure 3C–E). Levels of matrix metalloproteinase (MMP)-2 and MMP-9 enhanced in obstructed kidneys were also decreased with garcinol treatment at both days 3 and 7 after UUO (Figure 3F,G). Garcinol treatment also decreased the mRNA level of E-cadherin on day 7 after UUO (Figure 3H).

Garcinol decreased the renal mRNA level of vascular endothelial cadherin (VE-cadherin) at day 7 after UUO (Supplementary Figure S1A). It also decreased the levels of endothelial marker CD31 at day 3 post-UUO (Supplementary Figure S1B). Levels of tubular epithelial markers such as fibroblast-specific protein (FSP)-1 and galectin-3 that were elevated after UUO were also decreased at days 3 and 7 after garcinol treatment (Supplementary Figure S1C,D).

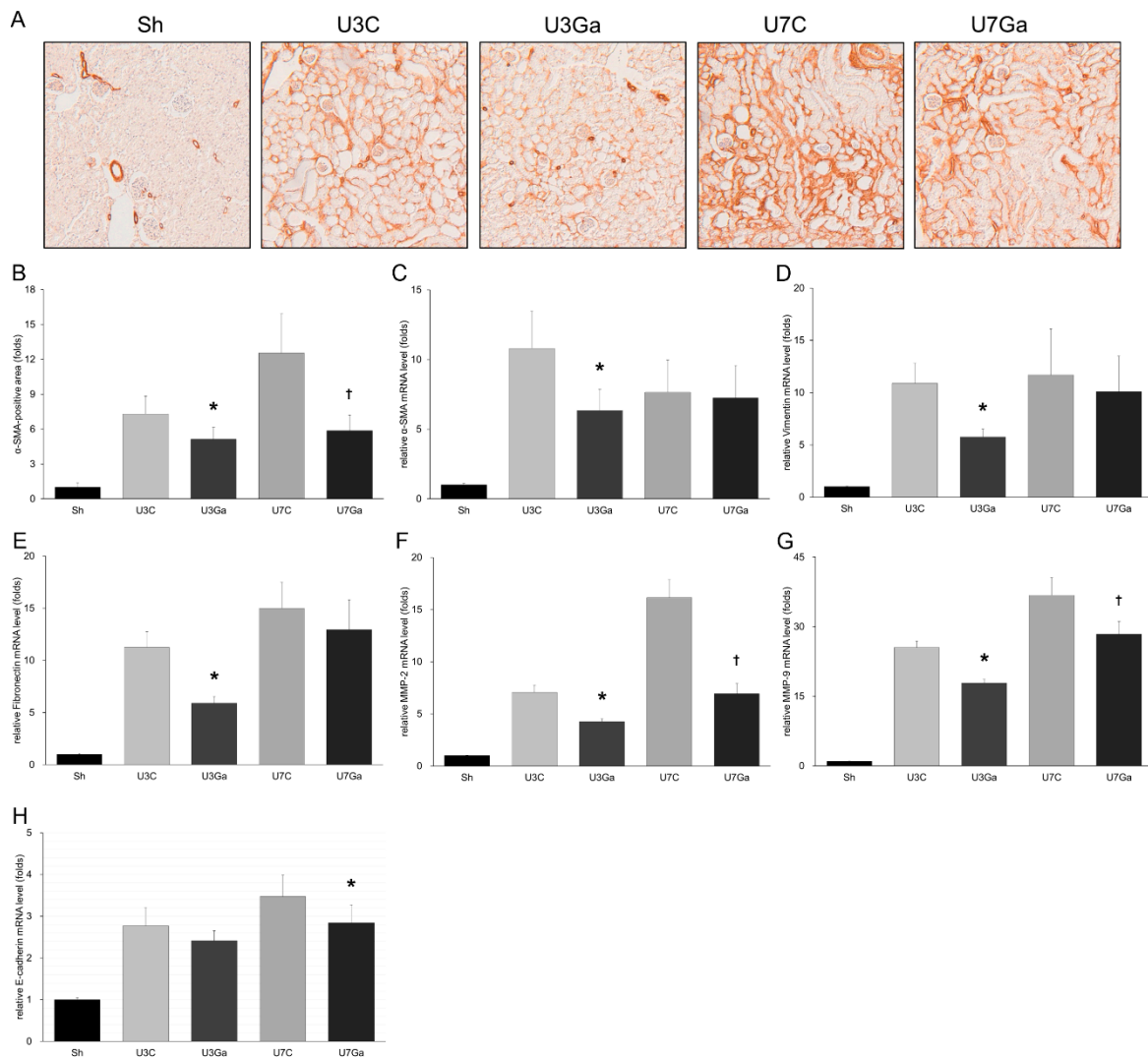


Figure 3. Effect of garcinol treatment on the renal expression of genes involving the epithelial-mesenchymal transition (EMT) pathway after UUO. (A,B) Immunostaining in the kidney showed that the accumulation of α -SMA after UUO was inhibited by garcinol treatment ((original magnification, $\times 200$). * $p = 0.002$ vs. U3C, † $p < 0.001$ vs. U7C. (C) qRT-PCR analysis of obstructed kidney tissue showed that the renal mRNA level of α -SMA was significantly decreased by garcinol treatment at day 3 after UUO. * $p < 0.001$ vs. U3C. (D,E) mRNA levels of vimentin and fibronectin were decreased by garcinol treatment at day 3 after UUO. * $p = 0.001$ vs. U3C. (F) MMP-2 mRNA levels were decreased by garcinol treatment at both day 3 and day 7 after UUO. * $p = 0.023$ vs. U3C, † $p = 0.004$ vs. U7C. (G) MMP-9 mRNA levels were decreased by garcinol treatment at both days 3 and 7 after UUO. * $p = 0.022$ vs. U3C, † $p = 0.001$ vs. U7C. (H) E-cadherin mRNA level increased after UUO was significantly decreased by garcinol treatment at day 7. * $p < 0.001$ vs. U7C.

2.4. Inhibition of PCAF Reduces Inflammation in Obstructed Kidneys

In UUO mice, F4/80-positive cells infiltrated the tubulointerstitium of the obstructed kidney (Figure 4A,B). After garcinol treatment, the number of F4/80 cells was significantly lower, indicating the inhibition of inflammation. Garcinol administration also significantly attenuated renal mRNA levels of interleukin (IL)-6 at day 7 after UUO and those of tumor necrosis factor (TNF)- α at days 3 and 7 post UUO (Figure 4C,D).

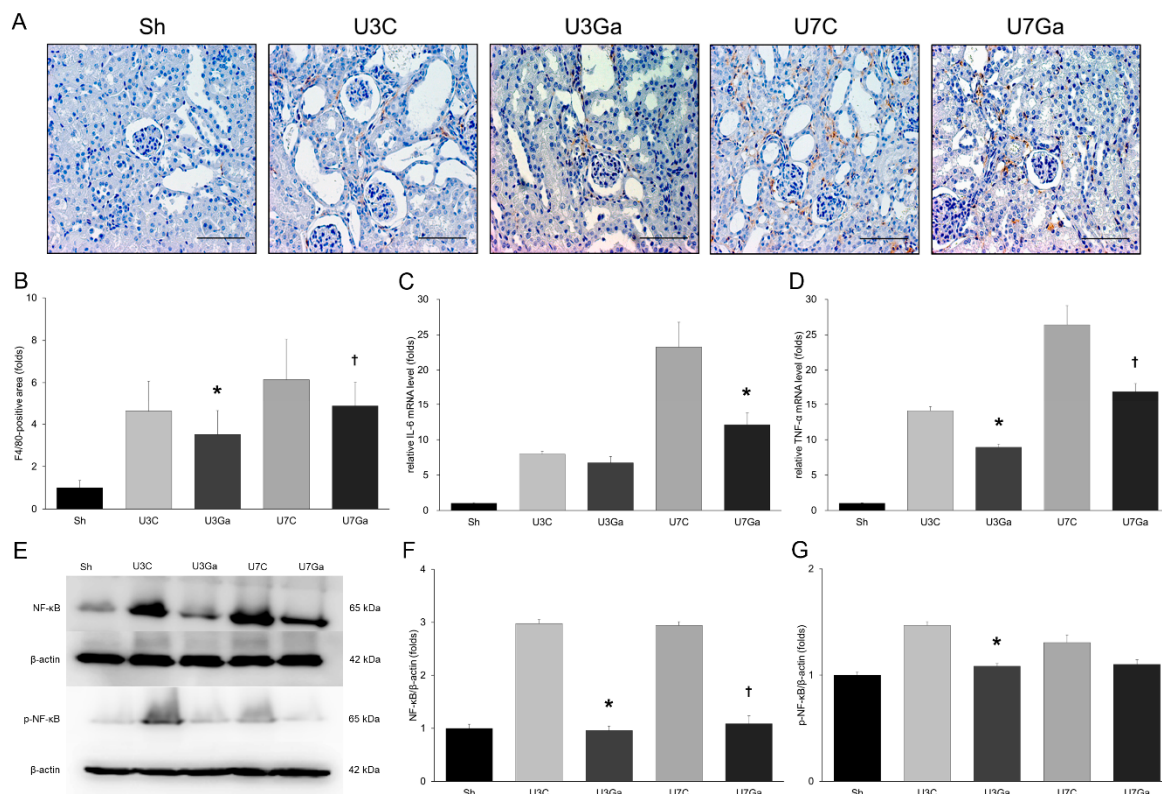


Figure 4. Effect of garcinol treatment on renal inflammation after UUO. (A,B) Immunohistochemistry staining showed that the number of F4/80-positive cells was increased by UUO, but decreased by the inhibition of PCAF (scale bar, 2 μ m). * $p = 0.016$ vs. U3C, † $p = 0.005$ vs. U7C. (C) qRT-PCR analysis showed that renal IL-6 level was decreased by garcinol treatment at 7 days after UUO. * $p = 0.029$ vs. U7C. (D) TNF- α mRNA level in UUO kidneys was significantly attenuated by garcinol. * $p < 0.001$ vs. U3C, † $p < 0.001$ vs. U7C. (E) Western blot for NF- κ B and p-NF- κ B. (F) Quantitative analysis showed that renal protein expression of NF- κ B was elevated by UUO, but significantly suppressed by garcinol treatment. * $p < 0.001$ vs. U3C, † $p < 0.001$ vs. U7C. (G) p-NF- κ B expression was reduced by garcinol treatment at day 3 after UUO. * $p = 0.001$ vs. U3C.

We then assessed the influence of a PCAF inhibitor on the important inflammatory response pathway NF- κ B. Increases in both NF- κ B p65 protein and its phosphorylation at Ser-536 were observed on days 3 and 7 after UUO (Figure 4E–G). This activation was significantly suppressed by garcinol treatment. Collectively, these results revealed that NF- κ B activation and the subsequent transcription of inflammatory genes after UUO were effectively inhibited by a PCAF inhibitor. This might be a mechanism underlying the anti-inflammatory effect of garcinol on renal fibrosis.

2.5. Inhibition of PCAF Decreases Oxidative Stress and Increases Antioxidant Enzymes in Obstructed Kidneys

It has been reported that oxidative stress contributes to the pathogenesis of UUO [13]. Thus, we examined the effect of the blockade of PCAF on renal oxidative stress. NADPH oxidases of the Nox family are the most prominent source of reactive oxygen species (ROS). The function of these enzymes is ROS generation [15]. Protein levels of Nox2 were markedly increased at both days 3 and 7 after obstructive injury. However, these increases were significantly attenuated by garcinol (Figure 5A,B).

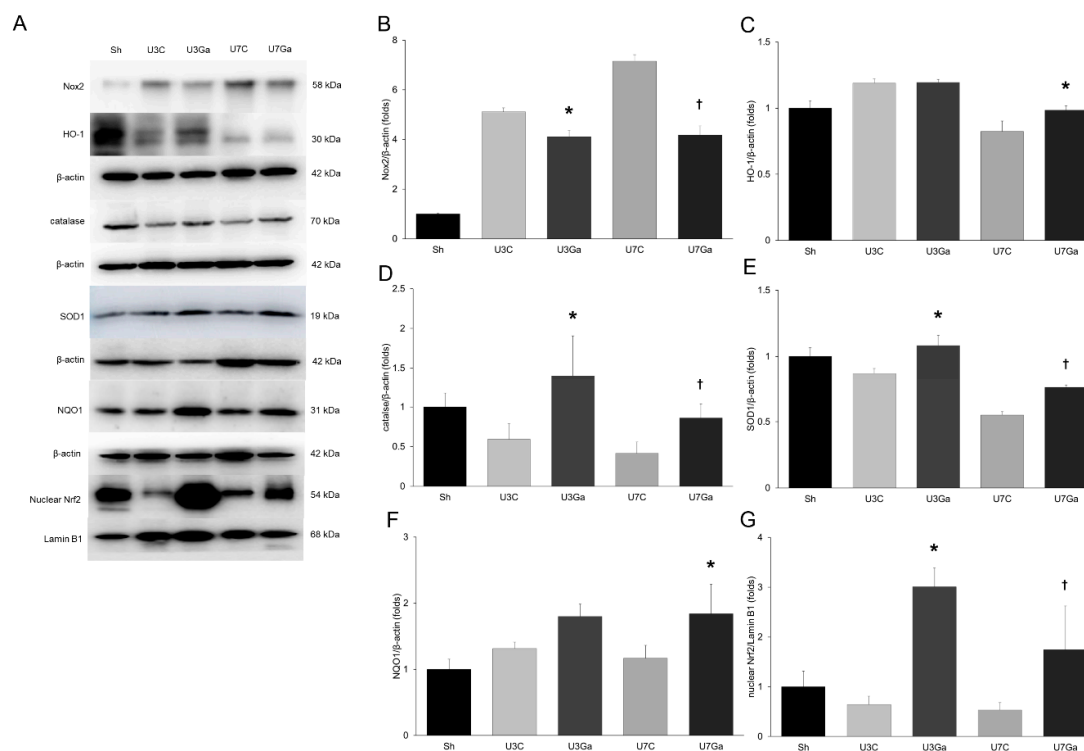


Figure 5. Effect of garcinol treatment on oxidative stress, antioxidant enzymes, and Nrf2 after UUO. (A) Western blot for Nox2, HO-1, catalase, SOD1, NQO1, and Nrf2. β -actin images were reused because the membranes for immunoblot analysis of CoI IV and TGF- β in Figure 2D were reprobbed with anti-Nox2 and HO-1, and with anti-catalase, respectively. (B) Quantitative analysis showed that the expression of Nox2 was increased after obstructive injury, but significantly decreased by garcinol at all timepoints. * $p = 0.015$ vs. U3C, † $p = 0.043$ vs. U7C. (C) Renal HO-1 expression in the obstructed kidneys was restored by garcinol treatment. * $p = 0.015$ vs. U7C. (D) Renal catalase expression in obstructed kidneys was increased by garcinol treatment. * $p < 0.001$ vs. U3C, † $p = 0.015$ vs. U7C. (E) Renal SOD1 expression in obstructed kidneys was restored by garcinol. * $p = 0.043$ vs. U3C, † $p = 0.018$ vs. U7C. (F) Renal NQO1 expression increased in the obstructed kidneys was further increased by garcinol treatment at day 7 post-UUO. * $p = 0.026$ vs. U7C. (G) Obstructive injury suppressed Nrf2 expression while garcinol treatment significantly increased its expression at all timepoints. * $p < 0.001$ vs. U3C, † $p = 0.013$ vs. U7C.

We also evaluated the expression of antioxidant enzymes. On day 7 after UUO, mice kidneys had suppressed expression of heme oxygenase-1 (HO-1). However, garcinol administration resulted in significantly increased expression of the HO-1 protein (Figure 5A,C). Protein expression levels of catalase and superoxide dismutase 1 (SOD1) decreased by UUO were also significantly restored by the administration of garcinol (Figure 5A,D,E). NAD(P)H:quinone oxidoreductase 1 (NQO1) demonstrated an increase after obstructive injury while garcinol was able to further increase its expression at all timepoints (Figure 5A,F). Given that these enzymes are major target genes of nuclear factor-erythroid-2-related factor 2 (Nrf2) [16], these results suggest that garcinol could affect Nrf2 activation. The expression of nuclear Nrf2 was decreased by UUO but was significantly increased by garcinol treatment (Figure 5A,G). These results indicate that inhibition of PCAF by garcinol could preserve the activation of Nrf2 and subsequent expression of its target genes.

2.6. Inhibition of PCAF Decreases Oxidative Stress and Increases Antioxidant Enzymes in Obstructed Kidneys

Considering that apoptosis was increased in the kidneys of mice with UUO, we determined the effect of garcinol on renal apoptosis by performing the terminal deoxynucleotidyl transferase dUTP nick end labeling (TUNEL) assay and Western blot for pro- and anti-apoptotic proteins. The number of TUNEL-positive cells was increased in the kidneys of UUO mice but was markedly decreased by garcinol treatment (Figure 6A,B). UUO caused a decrease in the ratio of Bcl-2 to Bax. This decrease was significantly increased by garcinol (Figure 6C,D).

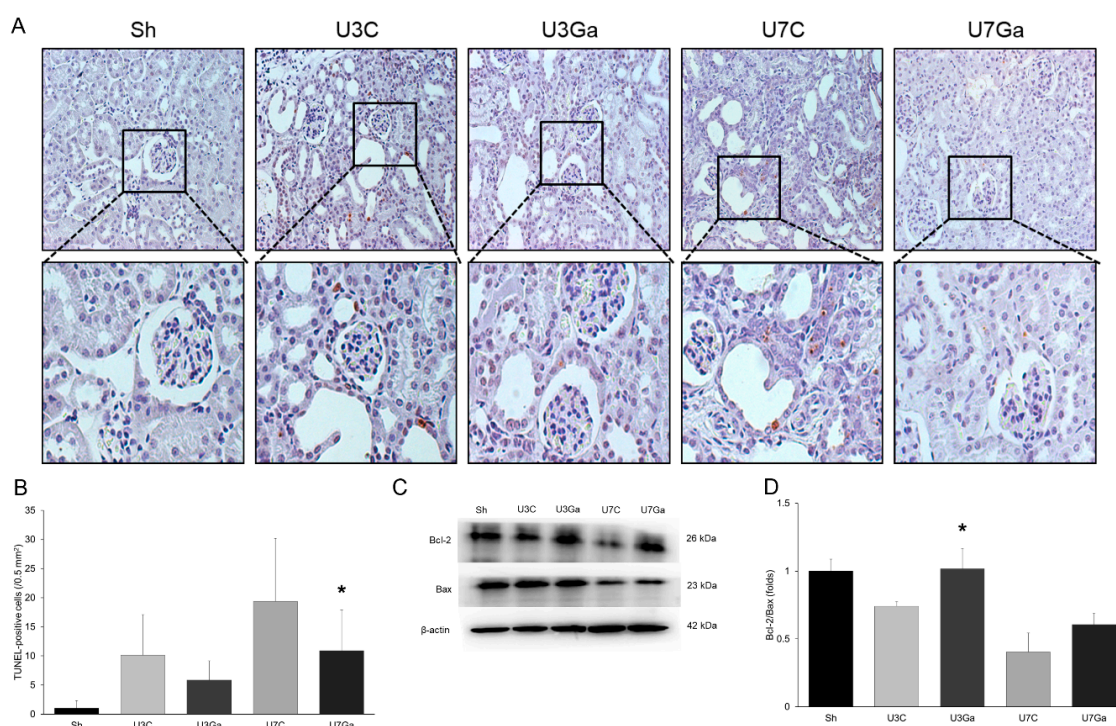


Figure 6. Effect of garcinol treatment on apoptosis after UUO. (A,B) Representative micrograph of TUNEL assay showed the increase of TUNEL-positive cells in the obstructed kidneys was decreased by garcinol (original magnification, $\times 200$). * $p < 0.001$ vs. U7C. (C,D) Western blot analysis showed that the ratio of the expression of Bcl-2 to that of Bax was increased by garcinol treatment. * $p = 0.021$ vs. U3C.

3. Discussion

The current study was designed to explore the role of PCAF in renal injuries induced by UUO. We showed that PCAF was substantially activated in nondiabetic kidneys undergoing renal inflammation and fibrosis. Our results indicate that PCAF might be able to simultaneously influence numerous mediators and signaling pathways of inflammation, oxidative stress, EMT, and apoptosis of diseased kidneys. Regarding the overall effects of PCAF on these processes, previous studies have primarily focused on the role of PCAF in inflammation.

By acetylating histone H3 or H4, histone acetyltransferases (HATs) such as CBP/p300 and PCAF can change the chromatin structure from heterochromatin to euchromatin, which facilitates the binding of transcriptional factors to promoters or enhancers in chromatin [17]. To be consistent with this hypothesis, CBP and PCAF are required for the transcriptional activity of NF- κ B, the central regulator of inflammation [9,18]. Moreover, the HAT activity of PCAF enhances the transcriptional activity of NF- κ B [19], suggesting that PCAF may play a critical role in inflammation by modulating the transcriptional activity of NF- κ B. In this study, the expression of proinflammatory cytokines including IL-6 and TNF- α , transcriptional target genes of NF- κ B, was upregulated associated with PCAF activation and as expected, the inhibition of PCAF activity with the treatment of garcinol reduced

the upregulation of pro-inflammatory cytokines, resulting in the prevention of renal fibrosis. Therefore, it can be hypothesized that harmful stimuli in the kidney such as UO activate PCAF activity as well as the NF- κ B signaling pathway, leading to pro-inflammatory gene expression, thus, the inhibition of the HAT activity of PCAF contributes to anti-inflammation, based on our results. Notably, garcinol treatment prevented the activation of NF- κ B (Figure 4), suggesting that PCAF might be involved in the activation pathway of NF- κ B. Although the mechanism of how PCAF is involved in the activation of NF- κ B in UO-induced renal fibrosis was not investigated in this study, this finding suggests that protein kinases or molecules regulating the activity of NF- κ B could be regulated by PCAF, as in the case of a virulence factor of *Yersinia*, YopJ, acetylating I κ B kinase (IKK) [20], which may highlight the feasibility of PCAF as a new therapeutic target in the pro-inflammatory process.

Another important finding in our study was that PCAF upregulation was associated with increased oxidative stress. Oxidative stress by elevation in ROS plays a pivotal role in renal fibrosis [21]. It is known that the balance between ROS production and the ROS scavenging system is an important homeostatic regulator in the progression of kidney fibrosis [21,22]. ROS produced by NADPH oxidases have been implicated in many physiologic and pathophysiologic processes. It plays an important role in cell signaling as a second messenger. It is known to mediate hormonal effects, regulate ion channel activity, oxygen sensing, adipocyte differentiation, gene expression, reproduction, cell growth, senescence, and apoptosis [22,23]. Furthermore, growing evidence indicates a role of NADPH oxidases in renal fibrosis [22]. In our experiment, elevated levels of renal Nox2 was downregulated in the kidneys of UO mice after treatment with garcinol. Although no studies have been published on the relationship between PCAF and Nox2, PCAF may play a role in the generation of ROS via Nox2 expression in the kidney. Oxidative stress is not only associated with the excessive production of ROS, but is also associated with disturbances in cellular antioxidant systems [24]. As described in previous findings [16,25], UO is linked to the reduced activity of antioxidant enzymes including HO-1, SOD1, and catalase. Genes encoding for these antioxidative proteins are transcribed by the activation of the Nrf2-Kelch-like ECH-associated protein 1 (Keap1)-antioxidant response elements (ARE) pathway [26]. Under a normal state, Nrf2 is retained by Keap1 in the cytoplasm [25,26]. With oxidative stress, Nrf2 will dissociate from Keap1 and translocate to the nucleus where it binds to ARE [26]. NF- κ B also regulates renal Nrf2 expression in the kidneys of CKD rats by promoting Keap1 and subsequent Nrf2 ubiquitination or interfering interaction of Nrf2 with ARE sequences [27,28]. Nrf2 is believed to be an anti-inflammatory modulator for the regulation of NF- κ B by decreasing I κ B α phosphorylation, thereby reducing the nuclear accumulation of NF- κ B [26,29]. In the present study, we found a decrease in nuclear Nrf2 and an increase in nuclear NF- κ B with the upregulation of PCAF in the kidneys of UO mice. After treatment with a PCAF inhibitor, there was an increase in the accumulation of nuclear Nrf2 and a subsequent increase in antioxidant enzymes as well as decreased accumulation of nuclear NF- κ B. These results suggest that PCAF is involved in the regulation of both the NF- κ B and Nrf2 pathways and that PCAF inhibition by garcinol may contribute to renoprotection by modulating the balance between inflammatory and antioxidant modulators.

In this study, we also evaluated the possible association between PCAF and EMT-related factors using both in vivo and in vitro experiments. Numerous factors can regulate EMT including growth factors, cytokines, hormones, and extracellular cues of different pathways [14,30]. Despite some debate on the contribution of EMT to renal fibrosis, it has been thought that EMT is an adaptive response of the epithelial following chronic injury that plays an integral role in the development of renal fibrosis [14,31]. During EMT, renal tubular cells lose their epithelial phenotypes evidenced by changes in epithelial markers such as E-cadherin and acquire new characteristic features of mesenchymal cells including increased expression of mesenchymal markers such as vimentin, fibronectin, MMP-2, and MMP-9 [31–34]. It has been reported that phosphorylation of upstream targets can influence the regulation of EMT-related factors [32,35]. For example, nuclear localization of NF- κ B through the phosphorylation of I κ B kinase- α and I κ B will in turn interact directly with the promoter of some EMT-related factors to regulate them at the transcriptional level [32]. Given that the exposure of cells to

garcinol significantly downregulates the expression of NF- κ B and inhibits its nuclear translocation [35], one possible mechanism by which PCAF regulates EMT would be through the control of NF- κ B.

The main limitation of this study was the absence of renal functional information. However, many previous studies have reported that BUN or serum creatinine is not significantly affected by UUO because of the presence of a contralateral kidney with good kidney function [36,37], indicating that BUN or serum creatinine is not a good indicator of renal function in an animal model of UUO [25]. In addition, although it would have been best for this study to separate the renal medulla from the renal cortex, all experiments were performed in whole kidneys. It has been reported that glomeruli initially remain viable by remodeling of Bowman's capsule after UUO and they could become non-functional with proximal tubular damage [38]. Cortical damage in the obstructive kidney was evidenced by a 50% reduction in the volume fraction of proximal tubular mass with unaltered relative mesangial area of glomeruli [39], suggesting that it would be justifiable to use whole kidney homogenates rather than medullary homogenates in this study.

In summary, we demonstrated that PCAF might play a major role in organizing whole fibrogenic processes through the modulation of inflammatory mediators, oxidative stress, and EMT. Garcinol treatment appears to appease excessively activated PCAF in diseased kidneys. It may correct the imbalance between activities of NF- κ B and Nrf2, driving decreased transcription of inflammatory mediators, and increased transcription of antioxidants. At the top-level of cellular processes, epigenetic mechanisms in chromatin can regulate gene expression, cellular identity, phenotypic variations, and disease states without altering the underlying DNA sequence [35]. For renal protection, epigenetic control of gene regulation might be a novel therapeutic strategy that could modulate many different pathological pathways simultaneously.

4. Materials and Methods

4.1. Animals

All experiments were performed in accordance with protocols approved by the Institutional Animal Care and Use Committee of The Catholic University of Korea, Yeouido St. Mary's Hospital (No. YEO20161601T). Male C57BL/6 mice weighing 20–25 g (OrientBio, Inc., Seoul, Korea) underwent left ureteral ligation with 4-0 silk thread under general anesthesia as described previously [16,29]. The sham operation was performed in a similar manner without ligation. Mice received an intraperitoneal injection of garcinol (Sigma-Aldrich Co., St. Louis, MO, USA) at 0.5 mg/kg/day or vehicle (200 μ L) alone at 3 or 7 days after operation. The dose of garcinol chosen in this study was expected to be non-toxic based on previous data [40,41]. Mice were divided into five groups (n = 6 per group): sham-operated control mice (Sh), control mice sacrificed on day 3 after UUO (U3C), garcinol-treated mice sacrificed on day 3 after UUO (U3Ga), control mice sacrificed on day 7 after UUO (U7C), and garcinol-treated mice sacrificed on day 7 after UUO (U7Ga). At the end of the experiment, kidneys were harvested for histological evaluation and molecular analysis.

4.2. Histology and Immunohistochemistry

As previously described [16,25], 4% phosphate-buffered paraformaldehyde-fixed kidney section was stained with Masson's trichrome to evaluate the severity of tubulointerstitial fibrosis. To assess the expression of PCAF (Abcam, Milton, Cambridge, UK) or H3K9ac (Abcam), kidney sections were reacted with the anti-PCAF antibody or anti-H3K9ac antibody followed by incubation with an anti-rabbit antibody (Vector Laboratories, Burlingame, CA, USA). To determine the extent of myofibroblasts or macrophages, sections were treated with anti- α -SMA or F4/80 (all from Abcam). After washing with PBS, all sections were incubated with peroxidase-conjugated anti-mouse IgG (Jackson ImmunoResearch Laboratories, West Grove, PA, USA) as a secondary antibody at room temperature for 90 min and then reacted with a mixture of 0.05% 3,3'-diaminobenzidine containing 0.01% H₂O₂ for color reactions. For quantitative assessment, more than 20 fields were randomly

selected and analyzed with MetaMorph image analysis software (Molecular Devices, Sunnyvale, CA, USA). To examine the degree of apoptosis, the TUNEL assay (Millipore, Billerica, MA, USA) was performed according to the manufacturer's protocol. TUNEL-positive cells were evaluated in 20 randomly selected tubulointerstitial fields for each section using ImageJ 1.49 software (National Institutes of Health, Bethesda, MD, USA). All histologic slides were assessed in a blinded manner.

4.3. Renal Collagen Content Assay

The total collagen content of kidney tissue was measured by acid hydrolysis of the kidney tissue as described previously [16,25]. Briefly, each kidney sample was hydrolyzed in 6 N HCl for 18 h at 110 °C and then dried at 75 °C. After solubilizing in a citric acid collagen buffer, samples were filtered through centrifugal filter units (EMD Millipore, Darmstadt, Germany) and then oxidized with chloramine-T solution. To start the color reaction, 100 µL of Ehrlich's reagent (Fisher Scientific, Fair Lawn, NJ, USA) was added. Sample absorbance was measured at 550 nm. Total collagen in the kidney tissue was calculated based on the assumption that collagen contained 12.7% hydroxyproline by weight.

4.4. Western Blot Analysis

Total proteins of kidney tissues were extracted using a PRO-PREP Protein Extraction Kit (iNtRON Biotechnology, Seongnam-si, Gyeonggi-do, Korea). Nuclear proteins of kidney tissues were extracted using a NE-PER Nuclear and Cytoplasmic Extraction Kit (Thermo Fisher Scientific, Waltham, MA, USA) according to the manufacturer's instructions. Protein concentrations were determined using a protein assay kit (Bio-Rad Laboratories, Hercules, CA, USA). After electrophoresis, proteins in the gel were transferred to a nitrocellulose membrane. The membrane was then incubated at 4 °C overnight with primary antibodies against the following proteins: PCAF (Abcam), Col IV (Abcam), TGF-β1 (Santa Cruz Biotechnology, Santa Cruz, CA, USA), NF-κB (Santa Cruz Biotechnology), phospho-NF-κB p65 (Ser-536, Cell Signaling Technology, Danvers, MA, USA), Nox2 (BD Bioscience, San Jose, CA, USA), HO-1 (Thermo Fisher, Waltham, MA, USA), catalase (Abcam), SOD1 (Enzo Life Science, Inc., Farmingdale, NY, USA), NQO1 (Santa Cruz Biotechnology), Nrf2 (Santa Cruz Biotechnology), Bcl-2, Bax (all from Santa Cruz Biotechnology), β-actin (Sigma-Aldrich, St. Louis, MO, USA), and lamin B1 (Cell Signaling Technology). After washing with PBS, blots were incubated with a secondary antibody conjugated with horseradish peroxidase. Protein bands were detected by enhanced chemiluminescence reagents and imaged using Image Quant LAS 4000 (GE Healthcare, Piscataway, NJ, USA). Band densities were determined with Quantity One 1-D analysis software (Bio-Rad Laboratories).

4.5. Quantitative Real-Time Polymerase Chain Reaction

Total RNA was isolated from the kidney tissues using TRIzol Reagent (Thermo Fisher Scientific) according to the manufacturer's manual. Reverse transcription was carried out to synthesize cDNA and qRT-PCR assays were performed using SYBR Premix (Takara Bio Inc., Otsu, Shiga, Japan). Primer sequences for each gene are listed in Table S1. The specificity of the PCR product was confirmed by analyzing the melting curve. All PCRs were performed in duplicate. Results were normalized to mRNA expression in the kidney tissues of sham-operated control mice.

4.6. Statistical Analysis

Values were represented as the mean ± standard error of the mean. Statistical differences between groups were determined using one-way analysis of variance with Bonferroni correction. In all analyses, $p < 0.05$ was considered statistically significant.

Supplementary Materials: Supplementary materials can be found at <http://www.mdpi.com/1422-0067/20/7/1554/s1>.

Author Contributions: Conceptualization, S.C. and H.-S.K.; experimental protocols, S.C., E.S.K. and H.-S.K.; data acquisition, S.K., M.S. and M.K.; data analysis and interpretation, S.C., S.K, S.J.S., C.W.P. and H.-S.K.; writing—original draft preparation, S.C.; writing—review and editing, S.C. and H.-S.K.; supervision, H.-S.K.; funding acquisition, S.C.

Funding: This research was supported by grants (NRF-2015R1C1A1A02037258 and NRF-2018R1A1A1A05020740) of the Basic Science Research Program through the National Research Foundation (NRF) funded by the Ministry of Science, ICT & Future Planning, Republic of Korea. It was also supported by a young investigator grant (2010) from The Korean Society of Nephrology.

Acknowledgments: The authors would like to thank Jong Hee Chung (Department of Statistics, Ewha Womans University, Seoul, Republic of Korea) for providing statistical advice.

Conflicts of Interest: The authors declare no conflict of interest.

Abbreviations

ARE	antioxidant response element
CBP	CREB binding protein
CKD	chronic kidney disease
Col IV	collagen IV
EMT	epithelial-mesenchymal transition
FSP-1	fibroblast-specific protein-1
GNAT	Gcn5-related N-acetyltransferase
H	histone
HAT	histone acetyltransferase
HDAC	histone deacetylase
HO-1	heme oxygenase-1
IL-1 β	interleukin-1 β
IL-6	Interleukin-6
I κ B α	nuclear factor of kappa light polypeptide gene enhancer in B-cells inhibitor, α
K	Lysine
Keap1	Kelch-like ECH-associated protein 1
LPS	lipopolysaccharide
MMP-2	matrix metalloproteinase-2
MMP-9	matrix metalloproteinase-9
MYST	MOZ, Ybf2 (Sas3), Sas2, and Tip60
NF- κ B	nuclear factor- κ B
NQO1	NAD(P)H:quinone oxidoreductase 1
NRC	nuclear coactivators
Nrf2	nuclear factor erythroid-derived 2-like factor 2
PCAF	p300/CBP-associated factor
qRT-PCR	quantitative real-time polymerase chain reaction
ROS	reactive oxygen species
SOD1	superoxide dismutase 1
TGF- β	transforming growth factor- β
TNF- α	tumor necrosis factor- α
TUNEL	terminal deoxynucleotidyl transferase dUTP nick end labeling
UUO	unilateral ureteral obstruction
VE-cadherin	vascular endothelial cadherin
α -SMA	α -smooth muscle actin

References

1. Gao, Y.; Tollefsbol, T.O. Impact of Epigenetic Dietary Components on Cancer through Histone Modifications. *Curr. Med. Chem.* **2015**, *22*, 2051–2064. [[CrossRef](#)] [[PubMed](#)]
2. Pandey, A.; Gaikwad, A.B. Compound 21 and Telmisartan combination mitigates type 2 diabetic nephropathy through amelioration of caspase mediated apoptosis. *Biochem. Biophys. Res. Commun.* **2017**, *487*, 827–833. [[CrossRef](#)] [[PubMed](#)]
3. Thorsheim, K.; Persson, A.; Siegbahn, A.; Tykesson, E.; Westergren-Thorsson, G.; Mani, K.; Ellervik, U. Disubstituted naphthyl β -D-xylopyranosides: Synthesis, GAG priming, and histone acetyltransferase (HAT) inhibition. *Glycoconj. J.* **2016**, *33*, 245–257. [[CrossRef](#)] [[PubMed](#)]
4. Pereira, C.P.; Bachli, E.B.; Schaer, D.J.; Schoedon, G. Transcriptome analysis revealed unique genes as targets for the anti-inflammatory action of activated protein C in human macrophages. *PLoS ONE* **2010**, *5*, e15353. [[CrossRef](#)] [[PubMed](#)]
5. Jing, Y.; Ai, Q.; Lin, L.; Dai, J.; Jia, M.; Zhou, D.; Che, Q.; Wan, J.; Jiang, R.; Zhang, L. Protective effects of garcinol in mice with lipopolysaccharide/D-galactosamine-induced apoptotic liver injury. *Int. Immunopharmacol.* **2014**, *19*, 373–380. [[CrossRef](#)]
6. Ghizzoni, M.; Boltjes, A.; Graaf, C.D.; Haisma, H.J.; Dekker, F.J. Improved inhibition of the histone acetyltransferase PCAF by an anacardic acid derivative. *Bioorg. Med. Chem.* **2010**, *18*, 5826–5834. [[CrossRef](#)] [[PubMed](#)]
7. Park, S.Y.; Lee, Y.H.; Seong, A.R.; Lee, J.; Jun, W.; Yoon, H.G. Selective inhibition of PCAF suppresses microglial-mediated β -amyloid neurotoxicity. *Int. J. Mol. Med.* **2013**, *32*, 469–475. [[CrossRef](#)]
8. Zhang, P.; Liu, Y.; Jin, C.; Zhang, M.; Lv, L.; Zhang, X.; Liu, H.; Zhou, Y. Histone H3K9 Acetyltransferase PCAF Is Essential for Osteogenic Differentiation Through Bone Morphogenetic Protein Signaling and May Be Involved in Osteoporosis. *Stem Cells* **2016**, *34*, 2332–2341. [[CrossRef](#)]
9. Zhao, J.; Gong, A.Y.; Zhou, R.; Liu, J.; Eischeid, A.N.; Chen, X.M. Downregulation of PCAF by miR-181a/b provides feedback regulation to TNF- α -induced transcription of proinflammatory genes in liver epithelial cells. *J. Immunol.* **2012**, *188*, 1266–1274. [[CrossRef](#)]
10. Lee, S.B.; Kalluri, R. Mechanistic connection between inflammation and fibrosis. *Kidney Int. Suppl.* **2010**, *S22–S26*. [[CrossRef](#)]
11. Huang, J.; Wan, D.; Li, J.; Chen, H.; Huang, K.; Zheng, L. Histone acetyltransferase PCAF regulates inflammatory molecules in the development of renal injury. *Epigenetics* **2015**, *10*, 62–72. [[CrossRef](#)] [[PubMed](#)]
12. Moriyama, T.; Kawada, N.; Nagatoya, K.; Takeji, M.; Horio, M.; Ando, A.; Imai, E.; Hori, M. Fluvastatin suppresses oxidative stress and fibrosis in the interstitium of mouse kidneys with unilateral ureteral obstruction. *Kidney Int.* **2001**, *59*, 2095–2103. [[CrossRef](#)] [[PubMed](#)]
13. Dendooven, A.; Ishola, D.A., Jr.; Nguyen, T.Q.; Van der Giezen, D.M.; Kok, R.J.; Goldschmeding, R.; Joles, J.A. Oxidative stress in obstructive nephropathy. *Int. J. Exp. Pathol.* **2011**, *92*, 202–210. [[CrossRef](#)]
14. Hung, T.W.; Tsai, J.P.; Lin, S.H.; Lee, C.H.; Hsieh, Y.H.; Chang, H.R. Pentraxin 3 Activates JNK Signaling and Regulates the Epithelial-To-Mesenchymal Transition in Renal Fibrosis. *Cell. Physiol. Biochem.* **2016**, *40*, 1029–1038. [[CrossRef](#)]
15. Babelova, A.; Avaniadi, D.; Jung, O.; Fork, C.; Beckmann, J.; Kosowski, J.; Weissmann, N.; Anilkumar, N.; Shah, A.M.; Schaefer, L.; et al. Role of Nox4 in murine models of kidney disease. *Free Radic. Biol. Med.* **2012**, *53*, 842–853. [[CrossRef](#)]
16. Chung, S.; Kim, S.; Kim, M.; Koh, E.S.; Yoon, H.E.; Kim, H.S.; Park, C.W.; Chang, Y.S.; Shin, S.J. T-type calcium channel blocker attenuates unilateral ureteral obstruction-induced renal interstitial fibrosis by activating the Nrf2 antioxidant pathway. *Am. J. Transl. Res.* **2016**, *8*, 4574–4585. [[PubMed](#)]
17. Steger, D.J.; Workman, J.L. Remodeling chromatin structures for transcription: What happens to the histones? *Bioessays* **1996**, *18*, 875–884. [[CrossRef](#)]
18. Vanden Berghe, W.; De Bosscher, K.; Boone, E.; Plaisance, S.; Haegeman, G. The nuclear factor-kappaB engages CBP/p300 and histone acetyltransferase activity for transcriptional activation of the interleukin-6 gene promoter. *J. Biol. Chem.* **1999**, *274*, 32091–32098. [[CrossRef](#)]
19. Sheppard, K.A.; Rose, D.W.; Haque, Z.K.; Kurokawa, R.; McNerney, E.; Westin, S.; Thanos, D.; Rosenfeld, M.G.; Glass, C.K.; Collins, T. Transcriptional activation by NF-kappaB requires multiple coactivators. *Mol. Cell. Biol.* **1999**, *19*, 6367–6378. [[CrossRef](#)]

20. Mittal, R.; Peak-Chew, S.Y.; McMahon, H.T. Acetylation of MEK2 and I kappa B kinase (IKK) activation loop residues by YopJ inhibits signaling. *Proc. Natl. Acad. Sci. USA* **2006**, *103*, 18574–18579. [[CrossRef](#)]
21. Jung, K.J.; Min, K.J.; Park, J.W.; Park, K.M.; Kwon, T.K. Carnosic acid attenuates unilateral ureteral obstruction-induced kidney fibrosis via inhibition of Akt-mediated Nox4 expression. *Free Radic. Biol. Med.* **2016**, *97*, 50–57. [[CrossRef](#)] [[PubMed](#)]
22. Sedeek, M.; Nasrallah, R.; Touyz, R.M.; Hébert, R.L. NADPH oxidases, reactive oxygen species, and the kidney: Friend and foe. *J. Am. Soc. Nephrol.* **2013**, *24*, 1512–1518. [[CrossRef](#)]
23. Rhee, E.P. NADPH Oxidase 4 at the Nexus of Diabetes, Reactive Oxygen Species, and Renal Metabolism. *J. Am. Soc. Nephrol.* **2016**, *27*, 337–339. [[CrossRef](#)]
24. Kim, J.I.; Noh, M.R.; Kim, K.Y.; Jang, H.S.; Kim, H.Y.; Park, K.M. Methionine sulfoxide reductase A deficiency exacerbates progression of kidney fibrosis induced by unilateral ureteral obstruction. *Free Radic. Biol. Med.* **2015**, *89*, 201–208. [[CrossRef](#)]
25. Chung, S.; Yoon, H.E.; Kim, S.J.; Kim, S.J.; Koh, E.S.; Hong, Y.A.; Park, C.W.; Chang, Y.S.; Shin, S.J. Oleanolic acid attenuates renal fibrosis in mice with unilateral ureteral obstruction via facilitating nuclear translocation of Nrf2. *Nutr. Metab.* **2014**, *11*, 2. [[CrossRef](#)] [[PubMed](#)]
26. Wang, Y.; Wang, B.; Du, F.; Su, X.; Sun, G.; Zhou, G.; Bian, X.; Liu, N. Epigallocatechin-3-Gallate Attenuates Oxidative Stress and Inflammation in Obstructive Nephropathy via NF- κ B and Nrf2/HO-1 Signalling Pathway Regulation. *Basic Clin. Pharmacol. Toxicol.* **2015**, *117*, 164–172. [[CrossRef](#)] [[PubMed](#)]
27. Bolati, D.; Shimizu, H.; Yisireyili, M.; Nishijima, F.; Niwa, T. Indoxyl sulfate, a uremic toxin, downregulates renal expression of Nrf2 through activation of NF- κ B. *BMC Nephrol.* **2015**, *14*, 56. [[CrossRef](#)]
28. Yu, M.; Li, H.; Liu, Q.; Liu, F.; Tang, L.; Li, C.; Yuan, Y.; Zhan, Y.; Xu, W.; Li, W.; et al. Nuclear factor p65 interacts with Keap1 to repress the Nrf2-ARE pathway. *Cell Signal.* **2011**, *23*, 883–892. [[CrossRef](#)]
29. Pedruzzi, L.M.; Stockler-Pinto, M.B.; Leite, M., Jr.; Mafra, D. Nrf2-keap1 system versus NF- κ B: The good and the evil in chronic kidney disease? *Biochimie* **2012**, *94*, 2461–2466. [[CrossRef](#)]
30. Hu, J.; Zhu, Q.; Li, P.L.; Wang, W.; Yi, F.; Li, N. Stem cell conditioned culture media attenuated albumin-induced epithelial-mesenchymal transition in renal tubular cells. *Cell. Physiol. Biochem.* **2015**, *35*, 1719–1728. [[CrossRef](#)]
31. Bai, Y.; Lu, H.; Lin, C.; Xu, Y.; Hu, D.; Liang, Y.; Hong, W.; Chen, B. Sonic hedgehog-mediated epithelial-mesenchymal transition in renal tubulointerstitial fibrosis. *Int. J. Mol. Med.* **2016**, *37*, 1317–1427. [[CrossRef](#)]
32. Kaufhold, S.; Bonavida, B. Central role of Snail1 in the regulation of EMT and resistance in cancer: A target for therapeutic intervention. *J. Exp. Clin. Cancer Res.* **2014**, *33*, 62. [[CrossRef](#)] [[PubMed](#)]
33. Lange-Sperandio, B.; Trautmann, A.; Eickelberg, O.; Jayachandran, A.; Oberle, S.; Schmidutz, F.; Rodenbeck, B.; Hömme, M.; Horuk, R.; Schaefer, F. Leukocytes induce epithelial to mesenchymal transition after unilateral ureteral obstruction in neonatal mice. *Am. J. Pathol.* **2007**, *171*, 861–871. [[CrossRef](#)]
34. Rhee, H.; Han, M.; Kim, S.S.; Kim, I.Y.; Lee, H.W.; Bae, S.S.; Ha, H.K.; Jung, E.S.; Lee, M.Y.; Seong, E.Y.; et al. The expression of two isoforms of matrix metalloproteinase-2 in aged mouse models of diabetes mellitus and chronic kidney disease. *Kidney Res. Clin. Pract.* **2018**, *37*, 222–229. [[CrossRef](#)] [[PubMed](#)]
35. Reddy, M.A.; Park, J.T.; Natarajan, R. Epigenetic modifications and diabetic nephropathy. *Kidney Res. Clin. Pract.* **2012**, *31*, 139–150. [[CrossRef](#)]
36. Ning, X.H.; Ge, X.F.; Cui, Y.; An, H.X. Ulinastatin inhibits unilateral ureteral obstruction-induced renal interstitial fibrosis in rats via transforming growth factor β (TGF- β)/Smad signalling pathways. *Int. Immunopharmacol.* **2013**, *15*, 406–413. [[CrossRef](#)]
37. Wu, W.P.; Chang, C.H.; Chiu, Y.T.; Ku, C.L.; Wen, M.C.; Shu, K.H.; Wu, M.J. A reduction of unilateral ureteral obstruction-induced renal fibrosis by a therapy combining valsartan with aliskiren. *Am. J. Physiol. Ren. Physiol.* **2010**, *299*, F929–F941. [[CrossRef](#)]
38. Forbes, M.S.; Thornhill, B.A.; Minor, J.J.; Gordon, K.A.; Galarreta, C.I.; Chevalier, R.L. Fight-or-flight: Murine unilateral ureteral obstruction causes extensive proximal tubular degeneration, collecting duct dilatation, and minimal fibrosis. *Am. J. Physiol. Ren. Physiol.* **2012**, *303*, F120–F129. [[CrossRef](#)] [[PubMed](#)]
39. Chaabane, W.; Praddaude, F.; Buleon, M.; Jaafar, A.; Vallet, M.; Rischmann, P.; Galarreta, C.I.; Chevalier, R.L.; Tack, I. Renal functional decline and glomerulotubular injury are arrested but not restored by release of unilateral ureteral obstruction (UUO). *Am. J. Physiol. Ren. Physiol.* **2013**, *304*, F432–F439. [[CrossRef](#)]

40. Sethi, G.; Chatterjee, S.; Rajendran, P.; Li, F.; Shanmugam, M.K.; Wong, K.F.; Kumar, A.P.; Senapati, P.; Behera, A.K.; Hui, K.M.; et al. Inhibition of STAT3 dimerization and acetylation by garcinol suppresses the growth of human hepatocellular carcinoma in vitro and in vivo. *Mol. Cancer* **2014**, *13*, 66. [[CrossRef](#)]
41. Li, F.; Shanmugam, M.K.; Siveen, K.S.; Wang, F.; Ong, T.H.; Loo, S.Y.; Swamy, M.M.; Mandal, S.; Kumar, A.P.; Goh, B.C.; et al. Garcinol sensitizes human head and neck carcinoma to cisplatin in a xenograft mouse model despite downregulation of proliferative biomarkers. *Oncotarget* **2015**, *6*, 5147–5163. [[CrossRef](#)] [[PubMed](#)]



© 2019 by the authors. Licensee MDPI, Basel, Switzerland. This article is an open access article distributed under the terms and conditions of the Creative Commons Attribution (CC BY) license (<http://creativecommons.org/licenses/by/4.0/>).